NUMERICAL STUDY OF VORTEX FLOW METERS

R. Belakroum #1 #2, T. H. Mai #1
#1 URCA/GRESPI/Laboratoire de Thermomécanique, Faculté des Sciences, BP 1039 51687 Reims Cedex 2, France

M. Kadja #2
#2 Laboratoire LEAP, Université Mentouri Constantine, Algérie

K. Zibouche #3
#3 Centre Scientifique et Technique du Bâtiment, 84, AV. J. JAURES PB02 77421 Marne-La-Vallée Cedex 2, France

ABSTRACT

This study relates to the flow meters which are widely used in industry for flow measurements. In a vortex meter occurs a phenomenon of vortex shedding which produces a periodic signal. The frequency of the latter is proportional to the volumetric flow rate. Through this numerical study we show the significant influence of the shape of the bluff body on the performances of these apparatuses. The stabilized finite element method known as GLS (Galerkin Least Squares) is used in order to simulate the flow of the fluid, assumed Newtonian and incompressible. For the modelling of turbulence we used the LES (Large Eddy Simulation) method.

The undertaken comparative study, relates to the obstacles having a section which can be square, triangular or in the shape of the letter T. The performances of the meters using each type of obstacle are checked numerically for different Reynolds numbers. A detailed attention is given to the step of time used in order to avoid numerical instability and also to be able to capture the low frequency of vortex shedding. For the calculation of Strouhal number we use the FFT method (Fast Fourier Transformation).

1. INTRODUCTION

The principle of operation of a vortex flow meter is based on a natural phenomenon known as Von Karman. In the wake of a bluff body placed in a flow of fluid, we observe the formation of vortices alternately. This phenomenon of vortex shedding results in a periodic signal of the pressure and velocity fields. If the shape of the bluff body is well appropriate, we find that there is a linear relationship between the frequency of vortices and flow velocity.

For a vortex flow meter the optimum would be to design a configuration where linearity between the frequency of vortex shedding and fluid flow velocity is satisfied for various fluids and a wide range of flow regimes.
This linearity is sensitive mainly to the form of the bluff body and to changes in the Reynolds number (Goujon-Durand, 1995).

The idea of designing a vortex shedding flowmeter was first proposed by Roshkol (Jiegang et al, 2004), who studied vortex shedding in the wake of a circular section cylinder. For this kind of bluff body, the temporal evolution of the formation of vortices in the wake zone is very sensitive to changes in flow regimes. In the case of sharp edges, the point of critical detachment is stable for a wide range of Reynolds number. For that reason, bluff bodies with sharp edges were adopted for the generation of vortices instead of a cylinder with a circular cross-section (Goujon-Durand, 1995).

The dimension of the bluff body is also important because it is preferable to be large enough to generate significant fluctuation in the wake region. However, the disadvantage of large size is congestion of ducts thus causing an immense loss in energy.

Recent research has explored vortex flow meters using increasingly small bluff bodies. Ultrasound techniques were used in these studies for the detection of vortex shedding and have shown great sensitivity to vortex frequency (Volker and Harald, 2003).

To improve the repetitive aspect and periodic behaviour of vortex shedding for the turbulent flow regimes, in their experimentation Bently et al (1996) introduced a second bluff body in series with the first. The recurrent vortex detachment is strong only in the case of some forms of obstruction. It is in this context that other experimental (Jiegang et al, 2004) and numerical (Yih-Jena, 2004) investigations were held in order to determine the optimal architecture of flow meters with vortex shedding.

This paper presents a comparative study of various forms of bluff bodies having a cross section which can be square, triangular or in the shape of the letter T. The performance of flow meters using each type of obstacles are checked for different Reynolds numbers. For each configuration, we calculated numerically the temporal evolution of the lift. Afterwards and using Fast Fourier Transformation the base frequency dominating vortex break-up is determined for each Reynolds number.

2. MATHEMATICAL FORMULATION AND NUMERICAL METHOD

2.1 Mathematical formulation

In this work, turbulence was modelled via the LES method (Large Eddy Simulation). This method uses the Smagorinsky model (Karamanos et all, 2000; Zibouche, 2005), which relates the turbulent viscosity to the mean velocity gradient by a length characterising the scales and thus filtering them.

The Reynolds equations for an unsteady flow of incompressible fluid are:

$$\frac{\partial U}{\partial t} + U \,.\, \nabla U - (\nu + \nu_t)\, \nabla\left(\nabla U + \nabla U^T\right) + \nabla P = f \quad \text{in } \Omega_f \text{ (t)} \qquad (1)$$

$$\nabla U = 0 \quad \text{in } \Omega_f \text{ (t)} \qquad (2)$$

where U, P, f and μ_t Are respectively flow velocity, pressure related to the density of the fluid, body(volume) forces and dynamic turbulent viscosity.

The turbulent viscosity is calculated using the following expression:

$$\nu_t = C_s\, h^2 \left| \sum_{ij} \left(\nabla U + \nabla U^T\right) \right| \qquad (3)$$

h is the local mesh size and C_s = 0,01 is the Smagorinsky constant.

The mechanical effect caused by the fluid flow on the body is made of three components: Fx and Fy acting in horizontal and vertical directions as well as the resulting moment M.

$$F = \int \left(-p + \nu \left(\nabla U + \nabla U^T\right)\right) \eta \, d\Gamma \qquad (4)$$

$$M = \int \left[-F_x (y - y_c) + F_Y (x - x_c) \right] d\Gamma \qquad (5)$$

Where $p, \nu, (x_c, y_c)$, Γ and η are respectively pressure related to the density of the fluid, kinematic viscosity, coordinates of the center of rotation, the contour of the bluff body and its external normal.

The dimensionless quantities corresponding to the resulting forces are the aerodynamic coefficients for drag, lift and moment.

$$C_x = \frac{2\, F_x}{\rho\, U_{\inf}^2\, D} \qquad (6)$$

$$C_y = \frac{2\, F_y}{\rho\, U_{\inf}^2\, D} \qquad (7)$$

$$C_m = \frac{2\, M}{\rho\, U_{\inf}^2\, D^2} \qquad (8)$$

The dimensionless quantity for the vortex shedding frequency is the Strouhal number:

$$S_t = \frac{f_{st}\, D}{U_{\inf}} \qquad (9)$$

Where $f_{st}, U_{\inf}$ and D are the frequency of vortex shedding, the velocity at the inlet and the height of the frontal surface to the flow.

2.2 Numerical method

The boundary conditions and the studied configuration are represented on Figure 1.

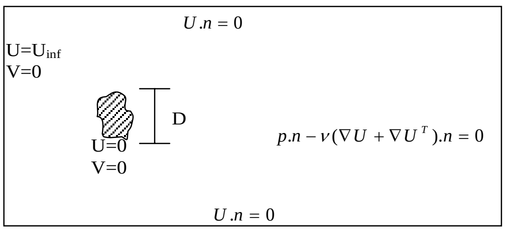

Figure 1: Studied configuration and boundary conditions

Because of the nonlinear nature of the problem under study, a linearization of the system of equations is required to be able to solve numerically the flow.

The term reflecting the convective transport $U.\nabla U$ is linearized as $U_k.\nabla U_{k+1}$ with the successive substitution method which is known to have a large convergence for the Navier-Stokes equation with the high Reynolds number.

The time derivative term is approximated by:

$$\frac{\partial U}{\partial t} = \frac{U^{n+1} - U^n}{\Delta t} \tag{10}$$

Where U^n and U^{n+1} are successively velocity at time steps t^n and t^{n+1}.

The discrete form of equations governing the flow is carried out by finite element method using the formulation stabilized type GLS (Galerkin Least Squares) (Zibouche, 2005). This formulation satisfies the LBB (Ladyzhenskaya - Babuska - Brezzi) condition. In addition it allows the use of hybrid element with equal interpolation order to the pressure and velocity (L. P. Franca et al, 1992).

The basic element that has been used is a mixed, triangular shape Lagrange P2/P1 and checking the condition inf-sup also called LBB condition (Donea and Huerta, 2003).

$$\int_{\Omega_f} \left(\frac{U}{\Delta t} + U_k \nabla U \right) v \, d\Omega \; +$$
$$\int_{\Omega_f} \nu_T \left(\nabla U + \nabla U^T \right) : \nabla v \, d\Omega - \int_{\Omega_f} P \, \nabla v \, d\Omega +$$
$$\sum_e \int_{\Omega_e} \tau^{GLS} \, [\left(\frac{U}{\Delta t} + U_k \, \nabla U \right) +$$
$$\nu_T \nabla \left(\nabla U + \nabla U^T \right) - \nabla P].[U_k \, \nabla v +$$
$$\nu_T \nabla \left(\nabla v + \nabla^T v \right) - \nabla q] \, d\Omega = \int_{\Omega_f} \left(f + \frac{U^n}{\Delta t} \right) v \, d\Omega$$
$$+ \sum_e \int_{\Omega_e} \tau^{GLS} \left(f + \frac{U^n}{\Delta t} \right) [U_k \, \nabla v + \nu_T \nabla \left(\nabla v + \nabla v^T \right)$$
$$- \nabla q] \, d\Omega \tag{11}$$

Fore the sake of clarity U_{k+1}^{n+1} is noted U. We also defined U^n as the velocity as previous time step t^n and U_k the velocity at the previous non-linear iteration.

$$\tau^{GLS} = \left[\left(\frac{2}{\Delta t} \right)^2 + \left(\frac{2\,U_h}{h_e} \right)^2 + \left(\frac{4\,\mu}{h_e^{\,2}} \right)^2 \right]^{-1/2} \tag{12}$$

$\nu_T = \nu + \nu_t$

h_e : The local size of the element

U_h : Local velocity

3. NUMERICAL RESULTS

In order to validate this numerical approach, we chose to compare our results primarily to those published by Okajima (1982) concerning the flow around a cylinder having a square section.

3.1 Analyses of the flow around a cylinder of square section

At time t = 25sec and a Reynolds number equal to 10^3 streamlines are represented on figure 2. The oscillations observed in the wake of the bluff body translated the phenomenon of vortex shedding which continued to occur in a perpetual and alternating manner in time.

The periodic aspect of this phenomenon is also reflected by the temporal evolution of the aerodynamic coefficients represented in Figure 3.

From the simulated values of the lift coefficient and by the use of the Fast Fourier Transform (FFT), one can deduce the base frequency dominating the phenomenon of vortex shedding. In figures 4 & 5 are represented two of the lift coefficient spectra corresponding to Re=10^3 and Re=10^4.

Figure 6 shows the variation of the Strouhal number as a function of the Reynolds number. The curve reflects a good agreement between the simulated and experimental values with a relative error whose peak reaches 9% for 6000 <Re <40000.

From Table 1, we can see that the simulated Strouhal numbers are underestimated by about 5%, as compared to the experimental values of Okajima (1982).

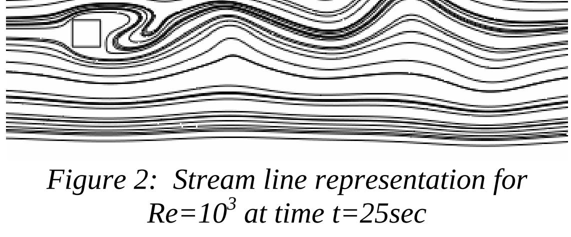

Figure 2: Stream line representation for Re=10^3 at time t=25sec

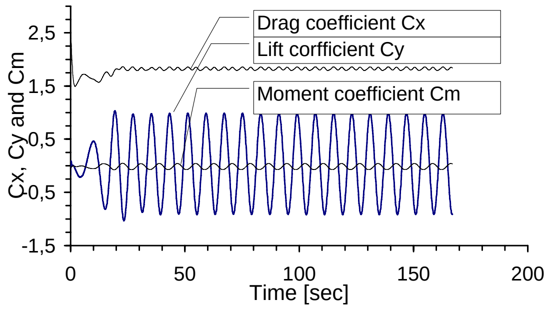

Figure 3: Time history of drag, lift and moment coefficients for Re=10^3

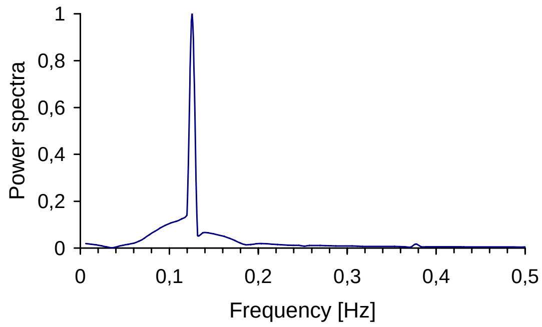

Figure 4: Representation of spectra corresponding to lift coefficient C_x for Re=10^3

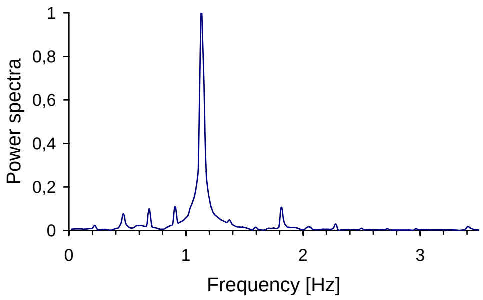

Figure 5: Representation of spectra corresponding to lift coefficient C_x for Re=10^4

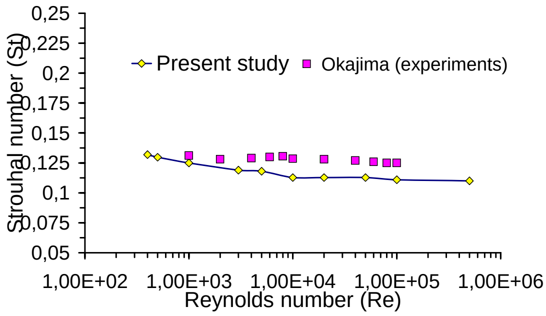

Figure 6: Present results compared to the experimental results of Okajima(1982).

Re	**Strouhal number** (reference value from Yih-Jena and Wen-Hann (2004))			
	Present study	Yih-jena (2004) (numerical) 0.04	Yih-jena (2004) (numerical) 0.01	Okajima (1982) (experimental)
100	**0.130**	0.139	0.144	0.135-0.140
200	**0.135**	0.148	0.152	0.140-0.148
250	**0.137**	0.148	0.151	0.140-0.148
300	**0.143**	0.147	0.149	0.139-0.140
400	**0.132**	0.144	0.138	0.130-0.135
500	**0.1298**			
1000	**0.125**			0.125-0.13

Table 1: Comparison of the simulated Strouhal number and the published results (square section)

3.2 Numerical prediction of the Strouhal number for different shapes of bluff body

Shapes of bluff body which are chosen to be analysed numerically are represented in figure 7 and are square, triangular and in shape of letter T. The evolution of the Strouhal number as a function of the Reynolds number is shown in Figure 8. For each form of bluff body the Strouhal number evolves in a different way.

For values of Re> 10^3 the Strouhal number is almost constant. This adheres perfectly with the results presented by Volker and Windorfer (2003). Therefore, the frequency of vortex shedding is proportional to the flow rate. Knowing the reference Strouhal number for each type of bluff body is therefore imperative for the effective design of vortex flow meters.

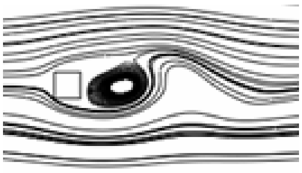

-a- *Square section*

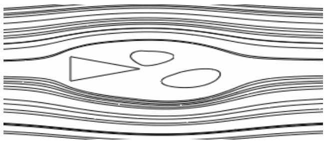

-b- *Triangular section first disposition*

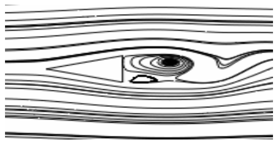

-c- *Triangular section second disposition*

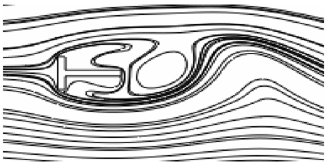

-d- *Shape of letter T (first disposition)*

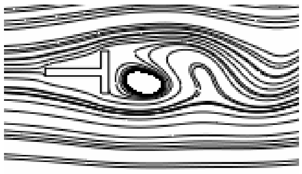

-e- *Shape of letter T (second disposition)*

Figure 7: Representation of different shapes of bluff body studied

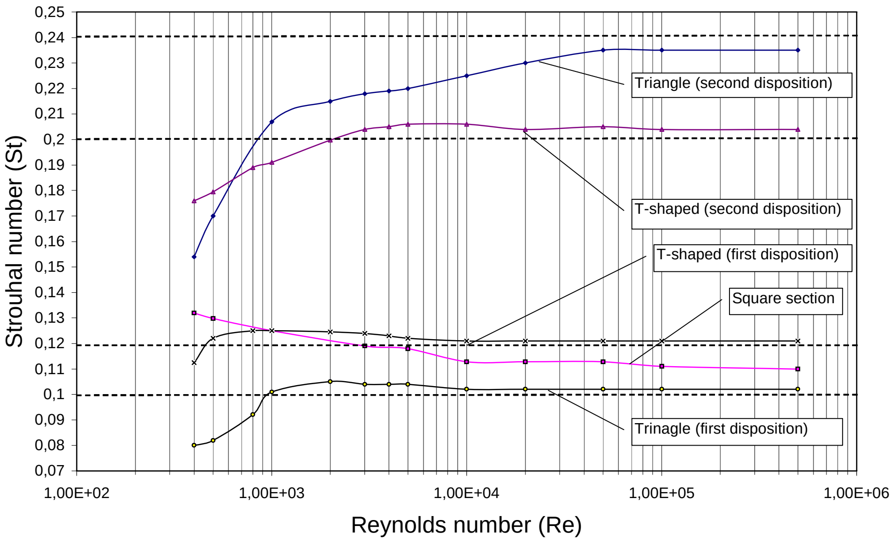

Figure 8: Variation of the Strouhal number according to Reynolds

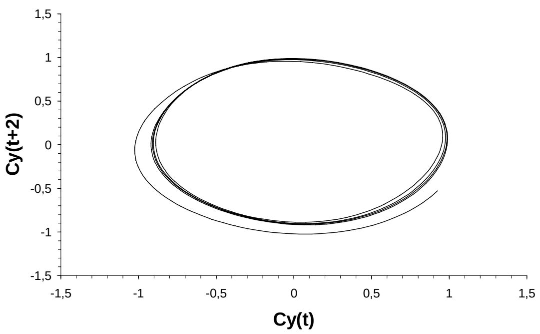

-a- *Square section*

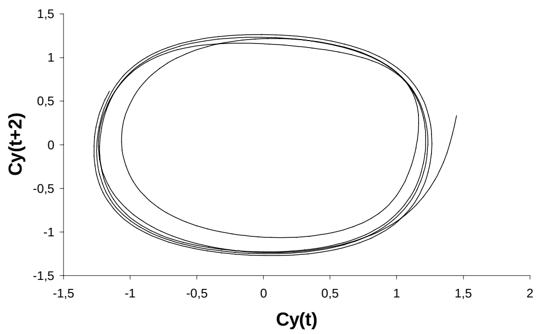

-b- *Section in the shape of the letter T (first disposition)*

Figure 9: Representation of Poincare sections for Re=10^3

Volker and Windorfer (2003) propose the following reference values:

- Triangular section (first disposition) St= 0,1
- Triangular Section (second disposition) St=0,24
- Section in the form of letter T (first disposition) St=0,2
- Section in the form of letter T (Second disposition) St=0.12

The constancy of the Strouhal number for great values of Reynolds is assured for all forms of bluff bodies used. However, for low flow regimes, the behaviour significantly differs from one shape to another. The optimal desired shape in the context of vortex flow meters is the one which disrupts in a minimal way the Strouhal number from its reference value. For this reason and from figure 8 we note that the square shape and the shape having the form of the letter T (first disposition) both are the most suitable.

In summary, in order to design an effective vortex flow meter, it is important to get a Strouhal number which is virtually constant regardless of the value of Reynolds number. It is also hoped that the vortex shedding signal obtained is the least polluted. It is known that the process is more or less random depending on the geometry studied as well as the flow regime. To better understand the phenomenon, we have plotted Poincare sections for the shapes having a square section and a section in the form of letter T. These are represented in figures 9(a) and (b). It can be inferred from these figures that for a value of the Reynolds number of 10^3, the signal of the lift is clearer in the case of a bluff body of square section.

4. CONCLUSION

For the design of a vortex flow meter we rely on certain linearity between the frequency of vortex shedding and flow rate. In other words on the constancy of the Strouhal number. However, this property is very sensitive to the shape of the bluff body and is valid only for quite high values of the Reynolds number.

By using the finite element method, we simulated the flow around several shapes of bluff bodies which are: square, triangular and in the form of letter T. From the temporal evolution of the lift for each configuration and using the fast Fourier transform (FFT), the base frequencies were determined. The evolution of Strouhal number has thus been determined as a function of the value of Reynolds number.

Shapes of bluff bodies that have proved the most suitable for possible use in vortex flow meters are the square shape and the shape in form of the letter T (first disposition). Then, using the plot obtained for Poincare sections, it has been estimated that the signal emitted by a bluff body of square section is less polluted.

It remains to be noted that other investigations are necessary to be able to better approximate an optimal architecture of a vortex flow meter.

5. REFERENCES

Bentley JP, Benson RA, Shanks AJ, 1996, The development of dual body vortex flowmeters. Flow Measure Instrum, 7(2):85-90.

Donea Jean and Antonio Huerta, 2003, Finite Element Methods for flow Problems, Wiley.

Goujon-Durand Sophie, 1995, Technical note Linearity of the Vortex meter as function of fluid viscosity, Flow. Meas., vol. 6, No. 3: 235-238

Jiegang Peng, Xin Fu, Ying Chen, 2004, Flow measurement by a new type vortex flowmeter of dual triangulate bluff body, Sensors and Actuators A 115: 53-59.

Karamanos G-S, G. E. Karniadakis, 2000, A Spectral Vanishing Method for Large-Eddy Similation, Journal of Computational Physics. 163: 22-50.

L.P Franca, S.L Frey, J.T.R Hughes, 1992, Stabilized finite element methods: I. Application to advective-diffusive model, Comput. Methods Appl. Mech Engrg 95: 253-276.

Okajima Atsushi, 1982, Strouhal numbers of rectangular cylinders, J. Fluid Mech., 123: 379-398.

Volker Hans, Harald Windorfer, 2003, Comparison of pressure and ultrasound measurements in vortex flow meters, Mesurement 33: 121-133.

Yih-Jena Jan, Tony Wen-Hann Sheu, 2004, A numerical confirmation of the dual vortex flowmeter design, Computers & fluids 33: 1157-1174.

Zibouche Kamel, 15 Décembre 2005, Simulation numérique des problèmes d’interactions fluide-structure appliqués au domaine du batiment et génie civil, thèse de doctorat, Université Paris 6 – Pierre et Marie Curie.